

MASTER

Received OCT 1

SEP 08 1986

Los Alamos National Laboratory is operated by the University of California for the United States Department of Energy under contract W-7405-ENG-36

TITLE: ON-LINE EXTRACTION EFFICIENCY ANALYSES FOR THE LOS ALAMOS
FREE-ELECTRON LASER

LA-UR--86-2983

DE86 015295

AUTHOR(S): Alex H. Lumpkin, P-15
Renee B. Feldman, AT-6

SUBMITTED TO Eighth International Free Electron Laser Conference
Glasgow, Scotland
September 1-5, 1986

DISCLAIMER

This report was prepared as an account of work sponsored by an agency of the United States Government. Neither the United States Government nor any agency thereof, nor any of their employees, makes any warranty, express or implied, or assumes any legal liability or responsibility for the accuracy, completeness, or usefulness of any information, apparatus, product, or process disclosed, or represents that its use would not infringe privately owned rights. Reference herein to any specific commercial product, process, or service by trade name, trademark, manufacturer, or otherwise does not necessarily constitute or imply its endorsement, recommendation, or favoring by the United States Government or any agency thereof. The views and opinions of authors expressed herein do not necessarily state or reflect those of the United States Government or any agency thereof.

By acceptance of this article the publisher recognizes that the U.S. Government retains a nonexclusive, royalty-free license to publish or reproduce the published form of this contribution or to allow others to do so, for U.S. Government purposes.

The Los Alamos National Laboratory requests that the publisher identify this article as work performed under the auspices of the U.S. Department of Energy.

Los Alamos Los Alamos National Laboratory
Los Alamos, New Mexico 87545

jsa

ON-LINE EXTRACTION EFFICIENCY ANALYSES FOR THE LOS ALAMOS FREE-ELECTRON LASER

Alex H. Lumpkin and Renee B. Feldman

Los Alamos National Laboratory
Los Alamos, NM 87545 USA

ABSTRACT

The on-line extraction efficiency analysis procedures for the Los Alamos Free-Electron Laser are described. The analyses are based on the measurement of the electron beam's energy spectrum as a function of time under lasing and nonlasing conditions. In the nongraphic, tuneup mode the procedure takes about six seconds, so at a 1 Hz repetition rate for the laser we can analyze one out of every six shots. If graphics output is desired, it is produced at a 20-s repetition rate. The tapered wiggler result for extraction efficiency, $\eta \sim 2\%$ is presented as an example.

I. INTRODUCTION

One of the most important performance parameters for a free-electron laser (FEL) is the evaluation of extraction efficiency. As optical powers have increased to a few GW in the resonant cavity, damage to optical components has made it more difficult to quantify transient cavity losses. The need for an on-line capability for optimizing the laser performance was identified at the end of the oscillator experiments that were reported previously [1-3]. During the past year at Los Alamos, we have implemented an on-line analysis capability for quantifying the extraction efficiency. The analyses are based on the measurement of the electron beam's energy spectra as a function of time under lasing and nonlasing conditions.

II. EXPERIMENTAL

The Los Alamos FEL is a mid-infrared ($\sim 10\mu$) oscillator driven by an electron linear accelerator which produces a relativistic, 20-MeV electron beam. The e-beam pulse train is 100 μ s in length and consists of ~ 2000 micropulses of 20-ps duration separated by 46 ns. As has been described previously [2,4] an auxiliary e-beam deflector system located after the wiggler section (but before the electron spectrometer) is used to convert the non-energy analysis direction of the focal plane into a time axis as illustrated in Fig. 1. Fused silica screens in the focal plane convert the electron beam energy into a visible image via the Cherenkov mechanism. A microchannel plate intensified vidicon camera views this scene

and records the three-dimensional information (energy, intensity, and time). Because of this deflection/streak technique, each video raster line from the intensified camera involving the focal plane converter screen corresponds to a different time slice of the macropulse.

In Fig. 2 sample images from the electron spectrometer in nonlasing and lasing conditions are shown. In the lasing image the faint streak of signal going towards lower energy (left) is generated by those electrons that participated in the lasing process and which lost different amounts of energy. Macropulse time flows from top to bottom of the image. Qualitatively, the presence of such a low energy electron beam distribution on the real-time monitor display in the control room is indicative of lasing. The next section will present the quantitative analysis procedures applied to such data.

III. ANALYSIS AND RESULTS

The on-line quantitative analysis task is simplified by the fact that only a single raster line from each data set that represents $\sim 10\mu\text{s}$ of time needs to be digitized to evaluate the extraction efficiency. Figure 3 schematically represents the hardware components involved: the electron spectrometer, the intensified vidicon camera, the video freeze frame unit, the digital video raster line selector, the Nicolet 2090 digitizing oscilloscope, the RS232 link at 9600 baud, and the IBM-XT personal computer (PC). Each calculation requires a camera dark current reference, a nonlasing electron spectrum reference, and the lasing electron spectrum. The camera reference is subtracted from both electron spectra files to initiate processing.

In the nongraphics, tuneup mode, the two reference samples are digitized in the Nicolet and files are created in the PC. Then, under the computer's control, the selected line of the lasing image is digitized, the digital data is transferred to the PC, and the extraction efficiency is calculated each six seconds. The analysis flow chart is given in Fig. 4a. The program language is a compiled BASIC. At a 1 Hz repetition rate for the FEL, we can analyse one out of every six shots. The parameter values are printed on the video display monitor.

For the full quantitative analysis mode with graphics [5], additional steps are involved as shown in Fig. 4b. In addition to the spectrometer dispersion curve correction file and the mapping of channel number to energy, correction files for the video camera transfer curve (the change in video signal out for the change in light level input) and for the converter screen efficiency must be applied. Figure 5 shows the video signal as a function of input signal. In this case we sent signals through the whole system by varying the electron beam current at the focal plane of the spectrometer. There seems to be a significant change in the slope of the

transfer curve at low light levels. This also causes a decrease in contrast for signal variations at low input levels in comparison to the higher input levels. Figure 6 shows the correction curve generated from Fig. 5 and illustrates also that the correction applied is larger where the contrast is lower. This correction will be seen to be critical to the proper evaluation of the weak signal in the lasing tail. The data samples were analysed by a separate program that uses several of the same subroutines for calculating the peak profile's area, centroid, and full width at half maximum of intensity (FWHM). The correction file is initially entered by the operator in the present mode of operation.

The amount of Cherenkov light generated in the screen that actually reaches the vidicon tube is dependent on several factors. Some of these factors are: the angle between the electron beam direction and the Suprasil screen plane, the scattering effectiveness of the frosted back surface of the screen, the attenuation of light by color centers within the Suprasil, the amount of η cracked hydrocarbons deposited on the screen, the viewing port transmittance, the light collecting optics, and any internal shading in the intensifier tube. The vidicon tube also may have a variable sensitivity to light across its surface. However, one total efficiency correction is obtained by scanning the electron beam across the energy axis (while the external deflector is running) by varying the analyzing magnet current. The nearby wall-current monitor provides a normalization factor for any variation in beam current to the spectrometer during the scans. Beam spot intensities are then evaluated along the screen surface by the peak area measurements. Figure 7 shows that in addition to the general roll-off in efficiency at the extremes of the field-of-view (FOV) due to the collecting lens, there is a depression in the efficiency curve near the center of the profile. This latter efficiency loss is attributed to color center defects in the fused silica screen created by the 20-MeV electron beam bombardment. There also appears to be a light-absorbing residue build-up from the cracking of hydrocarbons within the vacuum system. For the on-line analysis only a sample correction from the region of interest need be applied.

To test the evaluation procedure we simulated the sequences of obtaining the camera dark current reference, a nonlasing shot, and a lasing shot by taking two nonlasing shots about 20 seconds apart and treating the second one as if it were a lasing shot. The dark current reference is subtracted from both files and the energy centroids of the resultant energy profiles are calculated. The shift in energy centroid is calculated as a fraction of the initial ~ 20 -MeV energy. As shown in the flow chart (Fig. 4b), the program outputs a number of parameters

that can be used to assess the validity of the extraction efficiency calculation as well as the plots. Other parametric values reported include the energy FWHM of the two samples, the areas in the evaluation region, the ratio of the lasing area to the nonlasing area, the region of evaluation, the correction files applied, and the number of channels used in the sliding average. The ratio of areas, which checks the conservation of electron number, proved to be very useful. As seen in Fig. 8, the test case shows the areas are almost identical, and the energy jitter resulted in a simulated extraction efficiency, $\eta = -0.09\%$. The negative sign indicates the second shot (the simulated lasing) was actually higher in average energy than the reference.

The application of these techniques to the lasing conditions using the 12%-tapered wiggler is illustrated by the raw data plot in Fig. 9. One notes the area balance is quite poor, a 26% discrepancy, and $\eta = 1.3\%$. Because we could see the very long "lasing tail" in the image (such as Fig. 2b), we attributed the loss of electrons to the camera transfer curve (Figs. 5 and 6). This was tested by evaluating the count difference in the low intensity region. Figure 10 shows the final result of $\eta \approx 2\%$ with all corrections applied and the background-subtracted data smoothed by the sliding average routine. It is noted that the area ratio is now within a few percent of complete agreement!

The sensitivity of η to analysis parameter variation was considered. Table I shows the effects of energy analysis range selection and the correction files. Statistical fluctuations can present a problem if they are at the extremes (large moment arms) of the sampling region. We approximated the sources of extraction efficiency error as energy jitter (0.1%), statistical fluctuations (0.1-0.2%), and correction curves (0.2-0.3%) for tapered wiggler results with this data structure (low-intensity, low-energy tail). The final value for this 10- μ s data sample $\sim 60\mu$ s into the macropulse is $\eta = 2.0 \pm 0.4\%$ at the 1- σ error level.

IV. SUMMARY AND CONCLUSIONS

We now have on-line two robust routines: one provides fast calculations for tuneup and the other provides a quantitative evaluation of extraction efficiency with a graphics output. The nongraphics start-up code measures one out of every six shots. A decision was made to use the Tektronic video hard copier with 20-s repetition rate for the graphics output. Once the copier was accepted as the limiting factor, a compiled BASIC was chosen as the language because of its facility with graphics and communication ports. There was easily enough time for accessing the digitizing oscilloscope; for applying the measured screen

efficiency correction and measured camera transfer curve correction; for mapping of channel number to beam energy; for smoothing with sliding averages; for calculating and displaying results; and for hard copying. Our initial experiences with this on-line analysis technique have been encouraging. There are currently several operator actions that we would like to eventually automate and put under minicomputer control. Also, we expect to speed up the PC's performance with the addition of an "elevator board" so that the IBM XT can emulate and IBM AT. The abilities to track the extraction efficiency qualitatively on the television monitor in real-time and quantitatively with the on-line techniques were invaluable in our attaining this 2 percent extraction efficiency result reported earlier this year.

V. ACKNOWLEDGEMENTS

The authors are indebted to R. W. Warren and D. W. Feldman for their identifying the need for the on-line capability and to S. Apgar for his assistance in the operation of the external deflector.

REFERENCES

- [1.] Brian E. Newnam, et al., "Optical Performance of the Los Alamos Free-Electron Laser," IEEE Journal of Quantum Electronics, Vol. QE-21, No. 7, pp. 867-881, July 1985.
- [2.] Richard L. Sheffield, et al., "Electron-Beam Diagnostics and Results for the Los Alamos Free-Electron Laser," IEEE Journal of Quantum Electronics, Vol. QE-21, No. 7 pp. 895-903, July 1985.
- [3.] Roger W. Warren, Brian E. Newnam, and John C. Goldstein "Raman Spectra and the Los Alamos Free-Electron Laser," IEEE Journal of Quantum Electronics, Vol. QE-21, No. 7, pp. 882-888, July 1985.
- [4.] A. H. Lumpkin, et al., "Time-resolved Electron Beam Diagnostics for the Los Alamos Free-Electron Laser Oscillator Experiment," IEEE Trans. Nucl. Sci., Vol. NS-30, p. 3139, August 1983.
- [5.] Code FELGRAF, developed by R. B. Feldman, private communication, 1986.

Figure Captions

- Fig. 1.** A schematic view of the slow deflector and fused silica screen in the focal plane of the electron spectrometer.
- Fig. 2.** Sample images from the electron spectrometer focal plane for nonlasing and lasing conditions.
- Fig. 3.** Block diagram of the on-line extraction efficiency analysis system.
- Fig. 4.** Flow charts for the non-graphics (a) and graphics output (b) analysis sequences.
- Fig. 5.** The intensified video camera transfer curve.
- Fig. 6.** The video signal correction curve generated from Fig. 5.
- Fig. 7.** The screen efficiency correction as a function of energy position.
- Fig. 8.** Test case of procedures for extraction efficiency analysis using two nonlasing shots taken 20 seconds apart.
- Fig. 9.** Raw data plots of the electron spectra for the nonlasing-lasing (NL-L) example.
- Fig. 10.** Processed data plots of the electron spectra for the example in Fig. 9. All corrections have been applied and the data smoothed. The nonlasing (NL) and lasing (L) curves are indicated.

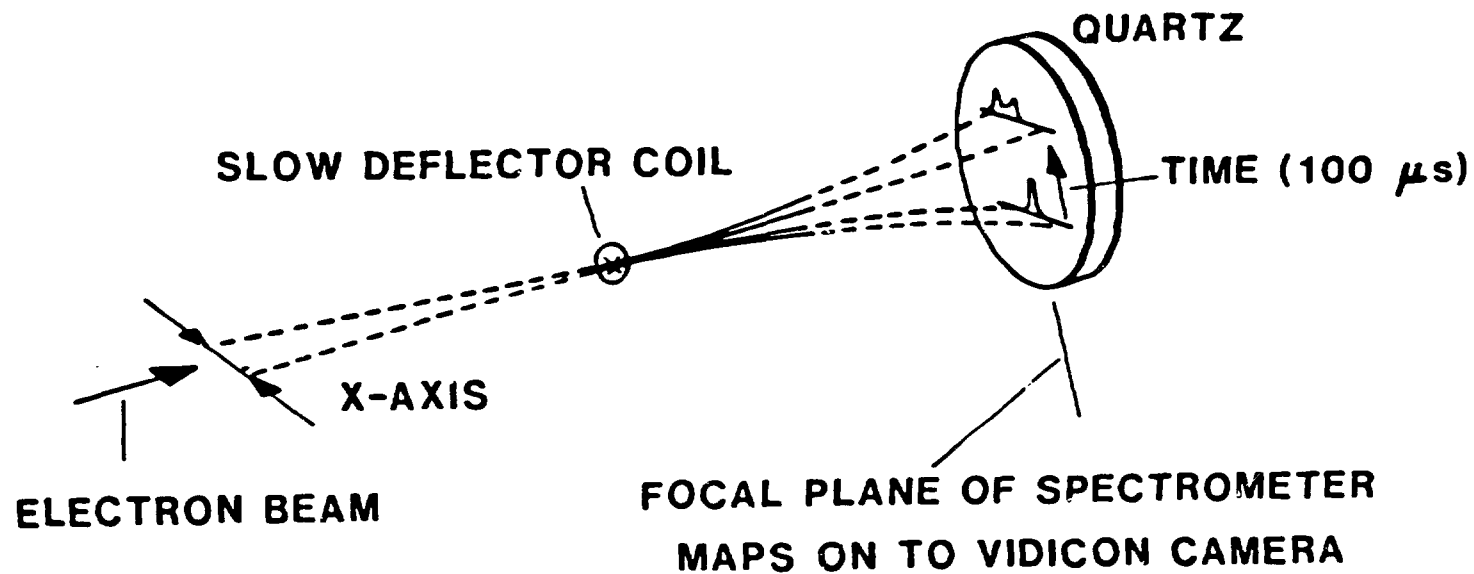
Table 1. Summary of extraction efficiency variation with analysis range and sliding average range. Other corrections were applied as indicated.^a

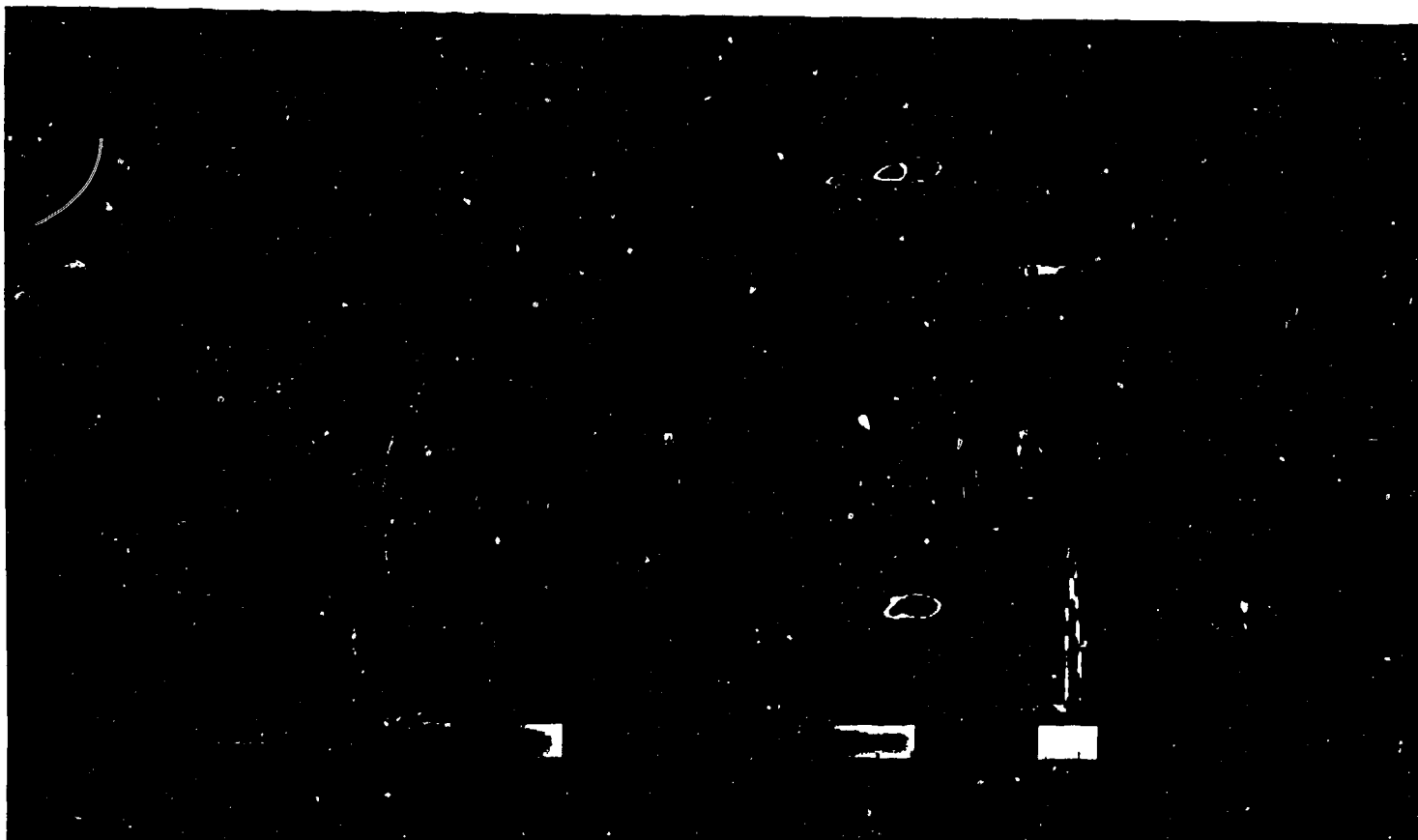
Case No.	Analysis Range Start Stop Channel# Channel#		Sliding Average Range (channels)	Area Ratio(L/NL)	η %
1	130	620	1	1.04	2.0
2	130	620	5	1.05	2.1
3	160	620	1	1.04	2.0
4	130	620	11	1.06	2.2
5	460	620	25	0.72	-0.3 ^b

a) Data of February 18, 1986; screen correction of February 14, 1986; and camera transfer correction of February 18, 1986.

b) Screen correction of February 10, 1986. The main point is 30% of the electrons are in the lasing tail which has not been included in the analysis range.

**COMBINATION OF BENDING MAGNET AND SLOW DEFLECTOR
PROVIDE 3-D PRESENTATION ON QUARTZ SCREEN**





REPRODUCED FROM
BEST AVAILABLE COPY

